Synthesis of Exfoliated Polyacrylonitrile/Na−MMT Nanocomposites via Emulsion Polymerization

Yeong Suk Choi, Ki Hyun Wang, Mingzhe Xu, and In Jae Chung*

Department of Chemical and Biomolecular Engineering, Korea Advanced Institute of Science and Technology (KAIST), 373-1, Guseong-dong, Yuseong-gu, Daejeon, Korea

Received November 7, 2001. Revised Manuscript Received April 5, 2002

Polyacrylonitrile/Na−MMT nanocomposites were synthesized through an emulsion polymerization of acrylonitrile (AN) using 2-acrylamido-2-methyl-1-propanesulfonic acid (AMPS). The silicate (Na−MMT) layers were exfoliated during polymerization. The nanocomposites were exfoliated up to 20 wt % content of pristine Na−MMT relative to the amount of AN and exhibited the enhanced storage modulus, *E′*, when compared with pure PAN. Delaminated morphology of the nanocomposite was confirmed by TEM.

Introduction

Organic/inorganic hybrids have mechanical properties of organic and inorganic materials showing and huge potential applications in electronics, adhesives, and automotive fields. Among various composites, engineers and researchers are focusing on polymer/silicate nanocomposites, expecting high stiffness,[2,3] strength, flame-retarding,[4−6] and gas barrier property even with small amount of silicate. These excellent properties result from the silicate layers dispersed in continuous polymers matrix. Two types of silicate nanocomposites are possible: intercalated and delaminated (or exfoliated). The Toyota group reported that nylon-6/silicate[2,3] nanocomposites showed enhanced modulus and strength without sacrificing other compensating property such as impact resistance. Since then, for the nanocomposites many polymers have been prepared: polystyrene,[8−10] poly(ethylene oxide),[11] polysiloxane,[12] poly(*n*-isopropylacrylamide),[13] polycarbonate,[14] urethane,[15] epoxy,[16,17] imide,[18] phenol,[19] resol,[20] polyethylene,[21] polypropylene,[22−24] and poly(methyl methacrylate).[25−27] But the research on polymer/silicate nanocomposite with homopolymers of polyacrylontrile[28−30] has been rare. Polyacrylonitrile (PAN)/silicate nanocomposites were synthesized by the in-situ polymerization of acrylonitrile with a smectite.[29] They showed the incomplete delamination of smectite. The polyacrylonitrile/hectorite nanocomposite[28] was also prepared by an in-situ hydrothermal crystallization method. The SAN (styrene−acrylonitrile copolymer)/montmorillonite nanocomposite was synthesized by Noh and co-workers,[31] and the basal space between the adjacent silicate layers became wide due to the intercalation morphology.

Natural silicates[1] have strong interaction between layers due to negative charges and hydrogen bond in their crystal structures. The basal space of pristine silicate is about 1 nm, which is smaller than the radius of gyration of general polymers. So general polymers may experience difficulties to penetrate into silicate layers, because of size and hydrophobic character of polymers. Therefore, organic modifiers are used to render the silicate layers hydrophobic and facilitate the

* To whom correspondence should be addressed: Telephone 82-42-869-3916, Fax 82-42-869-3910, e-mail chung@kaist.ac.kr.

(1) Pinnavaia, T. J. *Science* **1983**, *220*, 365.
(2) Usuki, A.; Kojima, Y.; Kawasumi, M.; Okada, A.; Fukushima, Y.; Kurauchi, T.; Kamigaito, O. *J. Mater. Res.* **1993**, *8*, 1179.
(3) Kojima, Y.; Usuki, A.; Kawasumi, M.; Okada, A.; Fukushima, Y.; Kurauchi, T.; Kamigaito, O. *J. Mater. Res.* **1993**, *8*, 1185.
(4) Gilman, J. W.; Jackson, C. L.; Morgan, A. B.; Harris, R., Jr.; Manias, E.; Giannelis, E. P.; Wuthenow, M.; Hilton, D.; Philips, S. H. *Chem. Mater.* **2000**, *12*, 1866.
(5) Gilman, J. W. *Appl. Clay Sci.* **1999**, *15*, 31.
(6) Hsiue, G. H.; Liu, Y. L.; Liao, H. H. *J. Polym. Sci., Part A: Polym. Chem.* **2001**, *39*, 986.
(7) Messersmith, P. B.; Giannelis, E. P. *J. Polym. Sci., Polym. Chem.* **1995**, *33*, 1047.
(8) Vaia, R. A.; Jaudt, K. D.; Kramer, E. J.; Giannelis, E. P. *Chem. Mater.* **1996**, *8*, 2628.
(9) Hoffmann, B.; Dietrich, C.; Thomann, R.; Friedrich, C.; Mülhaupt, R. *Macromol. Rapid Commun.* **2000**, *21*, 57.
(10) Lim, Y. T.; Park, O. O. *Macromol. Rapid Commun.* **2000**, *21*, 231.
(11) Sukpirom, N.; Lerner, M. M. *Chem. Mater.* **2001**, *13*, 2179.
(12) LeBaron, P.; Pinnavaia, T. J. *Chem. Mater.* **2001**, *13*, 3760.
(13) Liang, L.; Liu, J.; Gong, X. *Langmir* **2000**, *16*, 9895.
(14) Huang, X.; Lewis, S.; Brittain, W. J. *Macromolecules* **2000**, *33*, 2000.
(15) Wang, Z.; Pinnavaia, T. J. *Chem. Mater.* **1998**, *10*, 3769.
(16) Ishida, H.; Campbell, S.; Backwell, J. *Chem. Mater.* **2000**, *12*, 1260.
(17) Brown, J. M.; Curliss, D.; Vaia, R. A. *Chem. Mater.* **2000**, *12*, 3376.
(18) Tyan, H. L.; Leu, C. M.; Wei, K. H. *Chem. Mater.* **2001**, *13*, 222.
(19) Choi, M. H.; Chung, I. J.; Lee, J. D. *Chem. Mater.* **2000**, *12*, 2977.
(20) Byun, H. Y.; Choi, M. H.; Chung, I. J. *Chem. Mater.* **2001**, *13*, 4221.
(21) Bergman, J. S.; Chen, H.; Giannelis, E. P.; Thomas, M. G.; Coates, G. W. *Chem. Commun.* **1999**, 2179.
(22) Garćes, J. M.; Moll, D. J.; Bicerano, J.; Fibiger, R.; McLeod, D. G. *Adv. Mater.* **2000**, *12*, 1835.
(23) Galgali, G.; Ramesh, C.; Lele, A. *Macromolecules* **2001**, *34*, 852.
(24) Solomon, M. J.; Almusallam, A. S.; Seefeldt, K. F.; Somwangthanaroj, A.; Varadan, P. *Macromolecules* **2001**, *34*, 1864.
(25) Huang, X.; Brittain, W. J. *Macromolecules* **2001**, *34*, 3255.
(26) Zeng, C.; Lee, L. J. *Macromolecules* **2001**, *34*, 4098.
(27) Choi, Y. S.; Choi, M. H.; Wang, K. Y.; Kim, S. O.; Kim, Y. K.; Chung, I. J. *Macromolecules* **2001**, *34*, 8978.
(28) Carrado, K. A.; Xu, L. *Chem. Mater.* **1998**, *10*, 1440.
(29) Bastow, T.; Hardin, S. G.; Turney, T. W. *J. Mater. Sci.* **1991**, *26*, 1443.
(30) Bergaya, F.; Kooli, F.; Alcover, F. *J. Mater. Sci.* **1992**, *27*, 2180.
(31) Noh, M. H.; Jang, L. W.; Lee, D. C. *J. Appl. Polym. Sci.* **1999**, *74*, 179.

10.1021/cm0116020 CCC: $22.00
Published on Web 06/18/2002

penetration of polymers. But in our previous paper on the emulsion polymerization for the synthesis of PMMA/silicate nanocomposites,[27] we used water to make the basal space of silicate layers widen without any chemical treatment. We will extend this method to PAN and describe a simple and convenient way to obtain exfoliated PAN/Na−MMT nanocomposites through in-situ polymerization with 2-acrylamido-2-methyl-1-propanesulfonic acid (AMPS).[42−44] We will investigate their morphologies and mechanical properties.

Experimental Section

Materials. Acrylonitrile and 2-acrylamido-2-methyl-1-propanesulfonic acid (AMPS) were purchased from Aldrich and used as received. Sodium montmorillonite (Na−MMT) used in this paper was Kunipia-F of Kunimine Co. and had 119 mequiv/100 g of cation exchange capacity. Pristine Na−MMT was dispersed in deionized water for 12 h at an ambient temperature, before polymerization. Potassium persulfate (KPS) of Junsei, an initiator, was recrystallized using deionized water. *N*,*N*-Dimethylformamide (DMF) of HPLC solvent grade was used as received from Aldrich for polymer recovery in reverse ion exchange. Methyl alcohol (MeOH) of Fluka, a nonsolvent for PAN, was distilled at a normal pressure. Lithium chloride (Junsei) was recrystallized with THF.

Synthesis of PAN/Na−MMT Nanocomposites. Polymerizations were carried out in the following way with various amounts of Na−MMT. For example, Na−MMT dispersed in deionized water and a solution containing AN, AMPS, and deionized water with a ratio of 5 g/0.3 g/126 g (AN/AMPS/water) were charged into a 1000 mL four-neck reactor equipped with a baffle stirrer, a reflux condenser, a nitrogen inlet, and a rubber septum. The mixture was stirred at 200 rpm for 30 min under a N_2 gas at an ambient temperature. The temperature of the reactor was raised to 65 °C, and then 20 g of aqueous initiator solution (KPS = 1 wt %) was injected into the reactor via a glass syringe through a septum. Initial polymerization was performed at 65 °C for 1 h. The polymerization time was checked after the initiator injection to remove external factors affecting the polymerization, such as the increasing rate of temperature from room temperature to 65 °C and the stirring efficiency before the initiator injection. With Na−MMT, white particles were generated within 10 min after the initiator injection. In the absence of Na−MMT, white particles were formed in about 1 h. After the initial polymerization was completed, 15 g of AN was fed into the reactor through a septum with a syringe pump at the rate of 0.16 cm^3/min. After feeding monomer was completed, the reactor was kept at the same temperature to polymerize residual monomers for an additional 2 h.

Specimen for X-ray Diffraction Patterns. After freeze-dried for 5 days, a small amount of every nanocomposite was extracted to remove oligomers or water molecules by using a Soxhlet extraction apparatus with THF for 12 h, because small molecules may expand the interlayer space of Na−MMT, as if the polymers exfoliate the layers. The extracted nanocomposite was dried under a high vacuum at 50 °C for 50 h and molded in a shape of a disk at 3000 psi of pressure. Its basal space was calculated from the X-ray pattern.

To determine when the exfoliation occurs during the polymerization, reactant containing 5 wt % of Na−MMT was collected from the reactor at fixed time intervals. Every sample was freeze-dried for 5 days, dried further under a high vacuum at 50 °C for 1 day, and molded in the same way as the above for the X-ray pattern measurement.

Polymer Recovery by Reverse Ion Exchange.[7,27] After being freeze-dried, a small amount of nanocomposite was extracted with DMF/LiCl solution (60 g/0.2 g = DMF/LiCl) under a nitrogen atmosphere at 80 °C for 5 days in a 500 mL three-neck reactor fitted with a condenser, a nitrogen inlet, and an outlet. The mixture was centrifuged at 10 000 rpm for 30 min to separate polymers from the silicate cakes. The extract was filtered with a 0.45 μm membrane filter to remove clays or unwanted particles and poured into MeOH (10−20-fold) to precipitate PAN. The precipitated polymer was filtered and dried in a high vacuum at 80 °C for 50 h. Its molecular weight was measured with GPC.

Measurements. Infrared spectra were recorded on a Bomem 102 FT-IR spectrometer with KBR pellets. A total of 40 scans taken at 4 cm^{-1} of resolutions were averaged. X-ray diffraction patterns were obtained by using a Rigaku X-ray generator (Cu Kα with $\lambda = 0.154\,06$) with a scanning rate of 2°/min in a 2θ range of 1.5−10° at a room temperature. Number-average molecular weights were determined by using GPC. GPC analysis was performed at a flow rate of DMSO 2.0 mL/min at 80 °C using a Waters GPC system equipped with six styragel HR columns (two 500, two 10^3, 10^4, and 10^5) and a Water 410 RID detector after calibration with five polystyrene standards obtained from Polymer Laboratories. Thermogravimetric analyses (TGA) were carried out with a Perkin-Elmer thermobalance by heating from a room temperature to 700 °C with the rate of 10 °C/min under a N_2 atmosphere. Tan δ and storage modulus (E') were obtained by a Rheometric Scientific DMTA4 with a dual cantilever from 30 to 180 °C with a heating rate of 5 °C/min under 0.07% of deformation at 1 Hz of frequency. Samples were molded in 12 × 28 × 2 mm size at 140 °C for 2 min under 3000 psi of pressure. The glass transition temperature, T_g, was determined from the maximum value in the tan δ vs temperature scan. The morphology of the nanocomposite was examined by a Philips CM-20 transmission electron microscope. The nanocomposite was sliced in 100 nm thickness and coated with carbon. The accelerating voltage of TEM was 160 kV.

Results and Discussion

In the name of the sample, N denotes the monomer, acrylonitrile (AN), A stands for AMPS, and T stands for pristine Na-MMT, and the numbers following A and N indicate the weight of each component. Numbers next to T indicate the relative weight percentage of pristine Na−MMT to the weight of AN. For example, A0.3N20T10% nanocomposite includes AMPS of 0.3 g, AN of 20 g, and 10 wt % Na-MMT relative to 20 g of AN.

Figure 1 shows FT-IR spectra of Na−MMT, APMS, pure PAN, and A0.3N20T10%. The spectrum of A0.3N20T10% in Figure 1d contains characteristic absorbance bands of all components. C−H stretching at 2939 cm^{-1}, C≡N stretching at 2243 cm^{-1}, and C−H bending at 1454 cm^{-1} are the characteristic absorbance bands of PAN, and N−H bending at 1543 cm^{-1} and S=O stretching at 1369−1220 cm^{-1} are assigned to the vibration modes of AMPS. Absorbance peaks from O−H stretching at about 3624 cm^{-1}, Si−O stretching at about 1041 cm^{-1}, Al−O stretching at 628 cm^{-1}, and Si−O

(32) Svegliado, G.; Talamini, G.; Vidotto, G. *J. Polym. Sci., Part A-1* **1967**, *5*, 2875.
(33) Friedlander, H. N.; Peebles, L. H.; Brandup, J.; Kirby, J. R. *Macromolecules* **1968**, *1*, 79.
(34) Minagawa, M.; Iwamatsu, T. *J. Polym. Sci., Polym. Chem. Ed.* **1980**, *18*, 481.
(35) Minagawa, M.; Miyano, K.; Takahashi, M. *Macromolecules* **1988**, *21*, 2387.
(36) Minagawa, M.; Takasu, T.; Shinozaki, S. *Polymer* **1995**, *36*, 2343.
(37) Minagawa, M.; Onuma, H.; Ogita, T. Uchida, H. *J. Appl. Polym. Sci.* **2001**, *79*, 473.
(38) Ko, T. H.; Huang, L. C. *J. Appl. Polym. Sci.* **1998**, *70*, 2409.
(39) Thünemann, A.; Ruland, W. *Macromolecules* **2000**, *33*, 2626.
(40) Thünemann, A.; Ruland, W. *Macromolecules* **2000**, *33*, 1848.
(41) Viswanathan, H.; Wang, Y. Q.; Audi, A. A.; Allen, P. J.; Sherwood, P. M. A. *Chem. Mater.* **2001**, *13*, 1647.
(42) Seki, M.; Morishima, Y.; Kamachi, M. *Macromolecules* **1992**, *25*, 6540.
(43) Morishima, Y.; Nomura, S.; Ikeda, T.; Seki, M.; Kamachi, M. *Macromolecules* **1995**, *28*, 2874.
(44) Aota, H.; Akaki, S. I.; Morishima, Y.; Kamachi, M. *Macromolecules* **1997**, *30*, 4090.

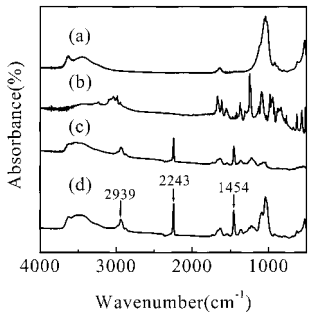

Figure 1. FT-IR spectra of (a) pristine Na−MMT, (b) reactive surfactant (AMPS), (c) A0.3N20T0%, and (d) A0.3N20T10%.

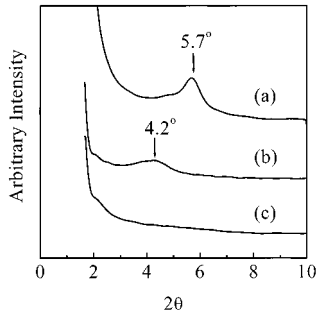

Figure 2. X-ray diffraction patterns of dispersions of pristine Na−MMT in water under various conditions: (a) the dispersion of Na−MMT in water, (b) with acrylonitrile (AN), and (c) the dispersion of Na−MMT in the aqueous solution of AN with AMPS.

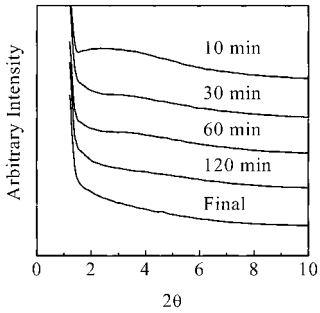

Figure 3. X-ray diffraction patterns of nanocomposites of A0.3N20T10% sampled at fixed time intervals during polymerization.

bending at 522 cm^{-1} confirm the presence of pristine Na−MMT in the nanocomposite.

Before the polymerization, the *d* spacing of Na−MMT layers was checked in various solutions. Figure 2 shows XRD diffraction patterns of (001) planes of Na−MMT in various water dispersions. In Figure 2a, the diffraction pattern of the (001) plane of Na−MMT dispersed in water occurs at 5.7° shifted by about 2° from its original position (7.7°) (in Figure 4), and its *d* spacing is 1.55 nm. It means that water molecules enlarge the basal space of Na−MMT. When monomer (AN) is added to this dispersion of Figure 2a, the diffraction of the (001) plane in Figure 2b appears at 4.2°, and its *d* spacing is 2.1 nm. The expansion of interlayer space of Na−MMT by monomer and water will facilitate the polymerization in the galleries of silicates. Furthermore, when the reactive surfactant is added to the dispersion of AN and silicates, the diffraction peak of Na−MMT in Figure 2c is rarely observable in the measurement range. In our previous paper on PMMA/Na−MMT nanocomposites,[27] the XRD diffraction pattern of Na−MMT dispersed in water with MMA and AMPS was not observable.

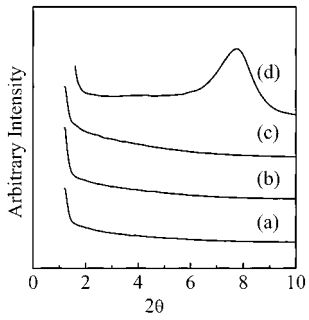

Figure 4. X-ray diffraction patterns of PAN/Na−MMT nanocomposites of (a) A0.3N20T5%, (b) A0.3N20T10%, and (c) A0.3N20T20%, extracted from THF for 12 h with a Soxhlet extraction apparatus. (d) The pattern of a pristine Na−MMT, a reference, and its pattern is measured by the powder method.

Table 1. Molecular Weights of PAN Recovered from PAN/Na−MMT Nanocomposites

PAN from each nanocomposite	M_n	M_w	PDI (M_w/M_n)
A0.3N20T0%	264 000	528 000	2.00
A0.3N20T5%	183 000	298 000	1.63
A0.3N20T10%	132 000	209 000	1.58
A0.3N20T20%	80 000	129 000	1.62

Figure 3 represents the variation in the basal space of A0.3N20T5% with time during polymerization. After 10 min of polymerization, a very broad diffraction pattern appears in a range of 1.5−5°, which indicates that the various basal spacings of Na−MMT are still present in the composite. As the polymerization goes on, the broad peak disappears gradually, and at least the peak is not observable. It infers that Na−MMT layers are exfoliated within 30 min after the initiation of polymerization initiated.

Figure 4 shows the X-ray diffraction patterns of nanocomposites after THF extraction for 12 h. Pristine Na−MMT has a diffraction peak of the (001) plane at 7.7° in a 2θ value, and its basal spacing is 1.14 nm. PAN/Na−MMT nanocomposites show no peak. It means the exfoliation of Na−MMT layers in a PAN matrix. In this experiment, the nanocomposite shows the exfoliated state up to 20 wt % of Na−MMT.

Molecular weights of PAN in nanocomposites are listed in Table 1. Number-average molecular weights (M_n) decrease as the amount of Na−MMT increases. It may be interpreted, as we discussed in the previous paper,[27] in the following way: AMPS and monomer are crowded around Na−MMT, and their local concentrations are high. This may affect the rate of polymerization. For a fixed amount of monomer, the concentrations of AMPS and monomer become lower as the amount of Na−MMT increases. So the number-average molecular weight of PAN become lower with the content of Na−MMT. Interestingly, the polydispersity index (PDI = M_w/M_n) of PAN shows a somewhat narrow distribution. In emulsion polymerization, usually PDI has a higher value than 2, which is caused by various possibilities of chain terminations, including the radical coupling with a reentering radical, the chain transfer by monomers, and the disproportionation.

Figure 5 shows thermogravimetric analysis (TGA) of the nanocomposites as a function of weight loss. Thermal decomposition of the polymer chain occurs about

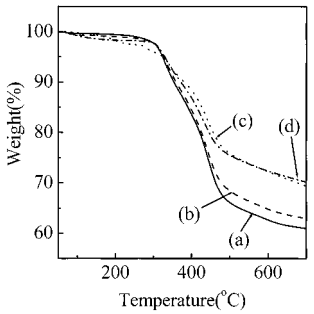

Figure 5. Thermal gravimetric curves for (a) A0.3N20T0%, (b) A0.3N20T5%, (c) A0.3N20T10%, and (d) A0.3N20T20% under a nitrogen atmosphere.

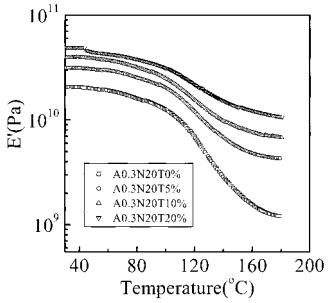

Figure 6. Dependence of storage modulus of (a) A0.3N20T0%, (b) A0.3N20T5%, (c) A0.3N20T10%, and (d) A0.3N20T20% on temperature. The storage modulus was measured by using DMA.

278−460 °C. In temperature range of 500−700 °C, a considerable amount of residue in the composite is observed, reaching a weight percentage of 61−70%. The high residual content may result from the formation of ring compounds, pyridinoid structures, which are precursors of carbon fibers.[38−41] Transformation of PAN to pyridinoid structures after TGA measurement was checked using FT-IR. Three new absorbance bands at about 1620−1500 cm^{-1} (C═C stretching), 1380−1267 cm^{-1} (C═N stretching), and 790 cm^{-1} (C−H out of plane) indicated the conversion of linear polymer chains in PAN into pyridinoid structures. The FT-IR spectrum is omitted here for simplicity.

The storage modulus, E', of nanocomposite increases with the amount of silicate as shown in Figure 6. At 40 °C, storage moduli are 2.0×10^{10} for pure PAN, 3.1×10^{10} for A0.3N20T5%, 4.0×10^{10} for A0.3N20T10%, and 5.0×10^{10} Pa for A0.3N20T10%. A0.3N20T5% shows a 55%, A0.3N20T10% a 100%, and A0.3N20T20% a 250% enhancement of storage modulus over pure PAN. In other nanocomposites, the major effect occurs less than 5% of silicate, but we observe the modulus increase up to 20 wt % of Na−MMT. We interpret that exfoliated morphology in the composite has the most strong effect on modulus increase. Pristine silicate and polarity of PAN also affect the enhancement because strong negative C≡N groups in PAN will interact with exfoliated layers of hydrophilic Na−MMT.

The glass transition temperature (T_g) of each nanocomposite is obtained from the maximum temperature of tan δ in Figure 7. Pure PAN and A0.3N20T5% have T_g at about 140 °C. For A0.3N20T10% and A0.3N20T20%, we do not observe the maximum value in tan δ and hence have lost the mobility like solids. If the molecules with a low molecular weight exist between the layers of silicate, the T_g becomes low with the

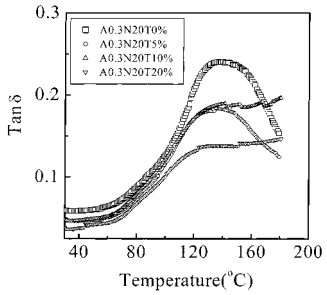

Figure 7. Tan δ of (a) A0.3N20T0%, (b) A0.3N20T5%, (c) A0.3N20T10%, and (d) A0.3N20T20% obtained by using DMA.

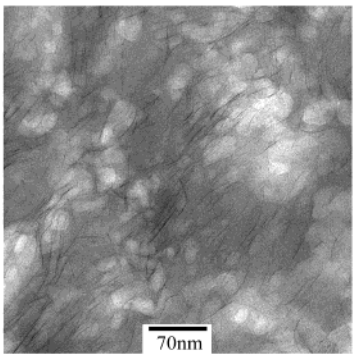

Figure 8. TEM micrograph of A0.3N20T10%.

increase in Na−MMT content.[27] The solidlike behavior of A0.3N20T10% and A0.3N20T20% may be explained this way. If Na−MMT layers are delaminated, the number of silicate sheets to contact polymer chains with will increase in a unit volume, and segmental motion of polymers in the composites will be strictly retarded by the delaminated Na−MMT layers. So the loss in mobility of molecules is observed.

TEM is used to confirm the morphology of nanocomposites in Figure 8, in which pristine Na−MMT layers look like dark strips, and PAN appears as white domains. Layers of Na−MMT in A0.3N20T10% are well distributed and delaminated, so the exfoliated morphology of Na−MMT is confirmed.

Conclusion

With a reactive surfactant, AMPS, containing amido portion and sulfonic acid, the exfoliated PAN/pristine Na−MMT nanocomposites were synthesized via an emulsion polymerization. The composites showed the exfoliated morphology up to 20 wt % of Na−MMT, and the exfoliation was confirmed by X-ray and TEM. They were exfoliated within 30 min after polymerization was initiated. With TGA analysis of nanocomposites, considerable amounts of residue were observed. The glass transition temperature of the nanocomposites was undetectable for A0.3N20T10% and A0.3N20T20%. Storage moduli of PAN/Na−MMT nanocomposites enhanced 55% for A0.3N20T5%, 100% for A0.3N20T10%, and 250% for A0.3N20T20% compared to pure PAN.

Acknowledgment. The authors express their sincere thanks to KOSEF (Korea Science and Engineering Foundation) and CAFPoly (Center for Advanced Functional Polymers) for their financial support.

CM0116020